



VIDEOMICROSCOPIC OBSERVATION OF NONEQUILIBRIUM GROWTH PATTERNS OF CRYSTALS

CHUNG-HSIEN TSAI(蔡政憲), TZE-JENG HSU(徐子正), and CHUNG-YUAN MOU*(牟中原)
Department of chemistry National Taiwan University Taipei, Taiwan.R.O.C.

We have developed a video-microscopic computer imaging system for observing meso-scale nonequilibrium physicochemical structures. Charged-coupled device (CCD) in optical detection, and computer-enhancement of digitized image, have greatly improved the resolution, sensitivity, and dynamical range of this technique. We apply this system to the observation of various complex crystallization patterns from Suberic acid melts and Camphene condensation. These patterns are of the scale one to 100 micrometers. They are resulted from nonlinear dynamical instabilities of a growing crystal fronts. The following patterns are observed: dendrites, destabilization of flat surface, cellular solidification, tip-splitting, and dense branches. A computer simulation based on diffusion-limited aggregates (DLA) model is performed to show this instability. The DLA model with surface tension effect is able to result in fractal-like, dendrite, and needle-like growth pattern.

INTRODUCTION

Optical microscopy (OM) is a powerful yet still under-exploited technique¹ for analyzing inhomogeneous chemical structure in liquid physicochemical system. In many applications, this was not very feasible in the past because the visual contrast between solvent and the structure is very low. The combining of optical microscopy with recent developments in computer imaging² has stimulated strong interest and many new discoveries in such disciplines as biology³, polymer physics⁴ and surface science⁵. Applications in the field of chemistry is just beginning; e.g. in the construction of two-dimensional spectrometer for observing chemical wave (B-Z reaction)^{6,7}. Recent advances in several fronts: charged-coupled device (CCD) in optical detection, and computer-enhancement of digitized image, have greatly improved the resolution, sensitivity, and dynamical range of this technique to the extent that quantitative analysis of 2-dimensional and 3-dimensional microscopic image becomes possible. For example, 3-D imaging properties of an fluorescence microscope have been quantitatively determined by combination of computer-manipulation of CCD imaging⁸. The idea is to use optical microscopy to determine its morphological properties in mesoscale (500 nm to 500000nm) so that fast and earlier

determination should be feasible. It is our purpose to develop such kind of digital video-microscopic system for observing mesoscale structures in physico-chemical systems. The system were applied to study phase transformations, emulsions, and chemical waves in liquid. In this paper, we will report our experimental system in detail and demonstrate the application in various nonequilibrium growth patterns in phase transformations.

An understanding of the origin of nonequilibrium structures such as snowflakes has long fascinated scientists. The dendrite structure is highly complex but ordered. It brings to us many basic questions. How do such intricate patterns come into being from apparently structureless liquid? When does nature make dendrite pattern instead of perfect solid crystal? What kind of growth kinetics is responsible for such delicate structures? Recently, there are strong interests from theoretical considerations of this problem⁹. We now basically understand the major theoretical ingredients of the process--the various factor involved in the instabilities of a growing crystal¹⁰--although there are still many details to be filled in. Surprisingly, there are not many experimental investigations in the origin of dendrite growth that are very relevant to the recent advances in theories in this field¹¹. Traditional studies of crystal growth have focused primarily on symmetry of atomic arrangement

or surface anisotropy. The formation of complex solidification patterns, however, has only been studied by metallurgists and material scientists from a more practical point of view. For systems with the scale of inhomogeneous pattern falls in the range of one to several hundred microns, a good microscopic system is needed to reveal its behavior. It is the purpose of this paper to demonstrate the newly developed computer-video-microscopic system can be applied to such system and observe many details of the non-equilibrium growth pattern. The observation shall assist further developments in theories.

THEORETICAL BACKGROUND OF PATTERN FORMATION IN CRYSTALLIZATION

There is a great variety of interfacial pattern formation in the growth between two phases. Though the morphology of the patterns formed in various physical system can be varied greatly, there are certain features that are common in the pattern growth processes. For complex pattern shape to grow, the system must be in the far-from-equilibrium state. System near equilibrium tends to be in the state of lowest free energy and consequently form simple geometrical structures dictated by its crystallographic symmetry group, simple polygon shape for example. When the system is driven out of equilibrium by some thermodynamic driving force, large supercooling for an example, the pattern can deform and the system is not able to relax to equilibrium structure in the process of growth. The global structure is determined by the requirement of dissipative process involved, hence it is sometimes called "dissipative structure". For the general cases of phase transformation, a key advance was the work of Mullin and Sekerka¹² from which they show that morphological instabilities are intrinsically kinetic in origin. That is, a system becomes linearly unstable against infinitesimally weak pattern-forming deformation, and that such thermal deformation can be much amplified into meso-scale structure. The fact that the growing interface has a curved structure is due to a morphological in-

stability of diffusionlimited growth, either thermal or material diffusion. Let us consider first the growth of a solid from pure melt. The latent heat released in the transformation warms the material near the solidification front and must be removed before further solidification can take place. If the solid develops an outward bump on an originally flat interface, the temperature gradient is larger there, since the solid surface will be at the same melting temperature and the supercooling temperature difference is applied across a shorter length. Consequently, the diffusion of latent heat away into the liquid phase is more rapid at the bump, and it grows faster there. If a bump becomes too sharp, however, it tends to melt back because of surface tension effect. The Gibbs-Thomson⁹ equation tells us that melting temperature of a solid is reduced by local curvature of the interface. The competition of the above stabilization and de-stabilization factors for a given system boundary condition largely dictates the global structure of this growing crystal. If the solid grows from a solution or a vapor, then the limiting dissipative mechanism is material diffusion. For either mechanism, the dynamics of the pattern growth can be described as a generalized Stefan problem¹⁰: the normal velocity of the growing interface v_n is proportional to the gradient of a scalar field u (either temperature or concentration) which satisfies the diffusion equation:

$$D \nabla^2 u = \partial u / \partial t \quad (1)$$

$$L v_n = c_p D \nabla u|_s \quad (2)$$

D is the diffusion constant, u is the diffusion field (concentration or temperature), L is the latent heat, and v_n is the normal velocity of the growing interface. The boundary condition at moving interface is given by⁹⁻¹²,

$$u(\text{surface}) = u_0 - k \kappa \quad (3)$$

where u_0 is the value of u for a flat surface given by phase equilibrium condition and κ is the local mean curvature of the interface. k is a constant that is related to surface tension. Equation (3) represents the correction to melting temperature due to surface curvature effect given by Gibbs-Thomson equation.

The solution of equation (1) to (3) can develop various kind of numerical instabilities that correspond to the ob-

served intricately curved interface pattern. It can also be simulated directly by random walk models. We will discuss the simulations in the last section.

EXPERIMENTAL

The experimental section is divided into two parts: in the first part, a digital video-microscopic system is described. In the second part, our method of obtaining image of crystallization pattern using the present system is described.

Digital Video-imaging system

There are two limitations to the use of optical microscopy in the characterization of microstructures of aggregates in liquids: contrast limitation and resolution limitation. The system is often of low contrast and difficult to be distinguished from background solvent with ordinary techniques. While optical techniques such as differential interference contrast⁹ do boost the contrast, one is still limited by the ability of eyes to distinguish small intensity difference since human eye is a logarithmic detector. This can be overcome by the combination of a CCD videocamera¹⁰, which is a multi-channel linear detector, and computer image processing techniques¹¹. One such manipulation is background subtraction of mottled pattern coming from lenses, the other is by gray-scale transformation. Assuming, for example, that the original image has gray-level between 120 and 140, the contrast can not be well resolved by human eyes. However, the computer can have the digitized image transformed into 256 gray-levels and use pseudo colors to further enhance the contrast. The discipline of image processing allows for other more complex mathematical manipulations of image: this includes filter operation, Laplace transformation, signal averaging by addition, statistical information on size and shape. Besides, light density profile over small scale can be obtained. All these techniques make the detection limit far lower than that of normal microscope. The apparent size limitation has been pushed

down to 50 nm.¹³⁻¹⁴ All the digital data manipulation can be done on a personal computer. With this equipment, it is expected that particle of size 0.1 micrometer can be clearly observed and motion on time scale greater than 1/30 second can be captured.

Figure 1 shows the optical and computer components of our digital image analysis system. The images are obtained with an Olympus BHS-313 microscope with Nomarski differential interference contrast (DIC) attachment polarizing or phase contrast microscope. Optical images are picked up by a Pulnix CCD video camera with high spatial resolution and they are digitized by a fast frame grabber (FG-100-AT, Imaging Technology) The images converted to video signal is fed to a high resolution color monitor (CD 233 Barco) or recorded in a video recording system if dynamical information is desired. The time resolution of the video system is 1/30 second per frame. Each image is represented by 512x512 pixel frame of 8-bit resolution and stored on RAM of the digitizer, or hard disk of the computer. The whole operation is controlled by an IBM/AT microcomputer. Slow-motion, fast-motion or image superposition can be done on computer. Final processed images are sent to image processor or to the color monitor for display which can be copied by a camera or a printer.

Many simple image enhancement and data manipulations can be done on the digitized image data file. Among them, contrast enhancement and line analysis are described

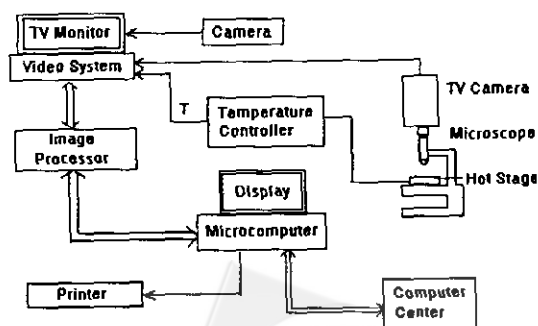


Fig.1. Schematics of Computer-enhanced Video-Microscopic System.

briefly here.

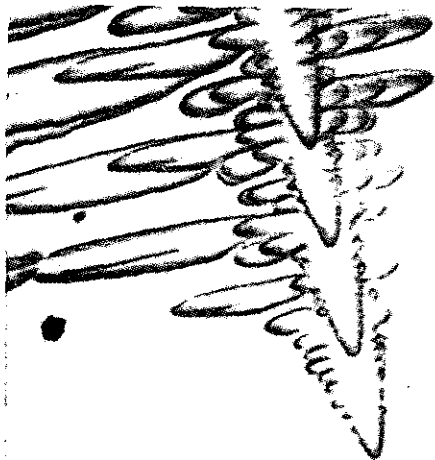
(1) Contrast enhancement: Although our DIC microscope enhances the contrast greatly already, the observation is still limited by the ability of eyes to distinguish small intensity difference for human eye is a logarithmic detector. As discussed in the introduction section, this can be overcome by the combination of a CCD videocamera¹³, which is a multi-channel linear detector, and computer image processing technique¹⁴.

(2) Line analysis - We can take a cross section of an image along any line and take its intensity profile. After Fourier transform, its power spectrum can reveal the periodicity of structure. This method is advantageous for studying periodic structures of dendrite or spherulite in crystal growth process.

Experimental method

For experiments on solidification from melt, we choose the substance to be Octanedioic acid (suberic acid) which has a melting point of 142°C. It is very soluble in water, so we assume there is small amount of impurity of water in the sample. The sample was not purified, since we would like to observe treelike crystal pattern and impurity would promote its formation. For experiments on sublimation, we choose Camphene; its melting point is 52°C.

The suberic acid sample is confined between micro-



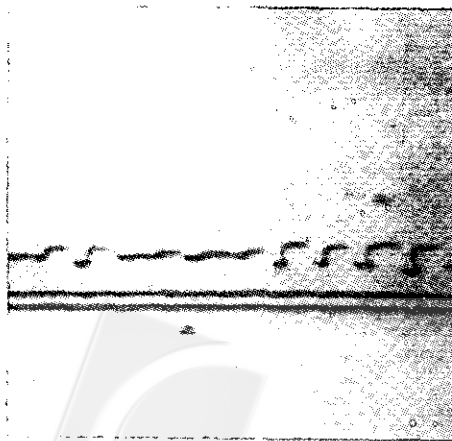
Picture 1. Superposition of time-lapsed photographs of a growing two dimensional dendritic crystal. (time interval of each exposure is 2 sec)

scopic slide and placed upon a thermally controlled hot-stage, which regulates the temperature within 0.1 K. The microscope is fitted with DIC and phase contrast optics. For sublimation experiment, the Camphene sample is placed in a horizontal UV-VIS absorption cell and heated from below by our hot stage. For the vapor condensation was observed on the other side of the cell, also by microscope.

The experimental procedure is as follows: starting from a crystallized state, the cell is heated to melt the substance at its melting point. Then it is cooled down to a temperature 0.3 to 5 degrees below the melting temperature. After a short transient time, one can observe dendrites growing from some nucleation site. For observing growth from flat surface, the system is kept at melting point with two coexisting phases stabilized for several minutes before the temperature is decreased suddenly. We follow the evolution of the system, restricting ourselves to the study of isolated subjects. The pictures are taken by a Minolta 7000i camera from monitor screen after the necessary image-processing procedures are performed.

RESULTS OF OBSERVATIONS

The various nonequilibrium shapes of the crystals obtained after quenching are shown in pictures 1 to 6. the features are explained as follows.



Picture 2. A sequence of the de-stabilization of flat surface process. (time: 0 sec, 8 sec and 31 sec)



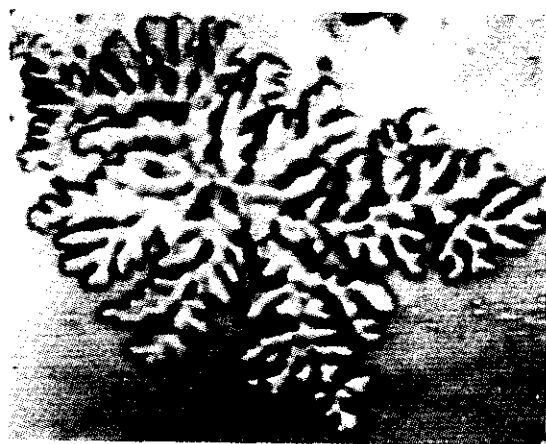
Picture 3. De-stabilization of flat surface with growing direction oblique to surface.



Picture 5. A sequence of superimposed images of cellular solidification. (time: 0 sec, 6 sec and 8 sec)



Picture 4. Tip-splitting and repressing effect of a fast-growing branch on the neighboring branch.



Picture 6. Dense branching pattern of vapor condensation of Camphene.

(1) Dendrite:

One of the most striking pattern is dendrite pattern; snowflake is the most well-known example. But a cleaner system from experimental point of view is a two-dimensional dendrite pattern as shown in Picture 1 of suberic acid. Nucleation occurs first and a cross-shaped micro-crystal is (not shown here) formed, then the four arms grows rapidly into a dendrite pattern. Picture 1 shows a time exposure sequence of four frames of suberic acid solid formed from a supercooled liquid. The principle characteristics are the

approximately constant velocity of growth (82 micrometers/sec for picture 1) and parabolic shape of the tip, and roughly evenly-spaced side branches. When the side-branches grow large enough there are secondary branches formed in side-branches. From the observation of many pictures of various supercooling, we found that the larger the supercooling the higher the velocity and the finer of the structure. We leave quantitative measurements of velocity, tip curvature, and side-branch size to a future paper. The physics underlying the growth of dendrite pattern is that suberic acid molecules attach continuously to a

microscopically rough surface and the rate is limited by the rate of diffusion of latent heat away from the interface.

(2) Destabilization of flat surface :

When supercooling is very slight and there is a flat interface to begin with, the flat surface can grow with a velocity less than 1 micrometer/sec and still maintain its shape. However, when the velocity exceeds 1 micrometer/sec, the flat surface de-stabilized into a tooth-shaped surface; and the bump part can grow faster. Picture 2 shows a sequence of the de-stabilization process, the solid part is at the bottom side. Because its sensitivity to temperature fluctuation, it is hard to obtain an even-spaced periodical structure. The bump in picture 2 is roughly perpendicular to the originally flat surface. In picture 3, the growing crystal direction is at an angle to the surface and the de-stabilization pattern becomes more complex. Picture 4 follows picture 3. In this picture, one can see the fast-growing branch has a repressing effect on the neighboring branch. Also notice that the tips are of parabolic shape.

(3) Tip Splitting:

The other striking phenomenon is the so-called tip-splitting. Both pictures 3 and 4 show this effect. In picture 4, this is clearly seen in the third branch, and in picture 3 this is also seen near the base of branches. This phenomenon is also observed in viscous-fingering process when a low-viscosity fluid is forced under pressure into a high-low-viscosity fluid. It is found that even when the two fluids are miscible, hence zero interfacial tension, there is still tipsplitting. Nittmann and Stanley¹⁵ explained that all these widely-different situations can be explained by the same set of equations (1) to (3). They occur by similar mechanism. First a cluster grows 'smoothly', without tip-splitting. However, as the radius of curvature increases, the interface becomes 'rough' in meso-scale, with both positive (outward) and negative (inward) fluctuations. The positive fluctuation soon damps out, whereas the negative fluctuation persist since it will protect the inlet formed (screening effect). The tiny notch formed will not likely be filled later.

(4) Cellular Solidification:

When the side-branch from a flat surface is closely

spaced, the rejection of impurity becomes a problem. The impurity concentration between the branches can exceed the equilibrium coexistence concentration at that temperature. Solidification process becomes concentration diffusion-controlled. And the de-stabilization leads to an array of cells, illustrated in picture 5. As in picture 3, if the drawing direction is not parallel to the crystal orientation, one observe a variety of oscillatory modulations. The velocity of growth is usually between those of dendrite growth and flat surface growth. The velocity for picture 5 is 22 micrometer/sec.

(5) Dense finger:

Picture 6 shows the result of vapor condensation of Camphene on a clean glass. The aggregation is the result of two-dimensional diffusion/condensation. In picture 6, the dense branching pattern of Camphene also exhibits tipsplitting. This result is very much like the viscosity-fingering pattern. Computer simulation by Nittmann and Stanley according to eq(1) to (3) also demonstrate this pattern. Actually, there are continuously distributed patterns between 'dense finger' and 'dendrite' patterns. When tip-splitting process dominates the system becomes 'dense finger'. On the other hand, when crystal anisotropy effects dominate the growth pattern becomes more like 'dendrite'. Computer simulations¹⁵ show that when molecular anisotropy is introduced, it can be amplified from its local molecular level into global effect at macroscopic level.

COMPUTER SIMULATIONS OF DENDRITE PATTERNS

As explained in equation (1), the pattern formation process in solidification is controlled by instabilities in the evolution of diffusion equation with time-dependent boundary condition, eq(2) and (3); they are called Laplace patterns.

Laplace patterns can be simulated by diffusion-limited aggregation model (DLA) originally introduced by Witten and Sander¹⁶ and modified by many workers¹⁷. In this

section we will use a modified version due to Witten and Sander¹⁸ will be used to simulate the growth of dendrite crystal growth pattern. The algorithm is very simple:

1. We create a square lattice of $N \times N$ size. At the center of the lattice, we put one crystal seed.
2. Release a random walker (Brownian particle) from peripheral at large radius in random direction.
3. The particle executes random walk along the square lattice.
4. Whenever the particle hits the seed or part of the crystal, it sticks at the position of impact with probability

$$p = \alpha^{3-B} \quad (4)$$

where α is an adjustable parameter between one and zero and B is the number of nearest neighbor at the position of impact. Ordinary DLA corresponds to $\alpha = 1$. Equation (4) is used to simulate surface tension effect, that is, molecules tend to aggregate into bulk such that it has larger radius of curvature.

5. Continue the release of the next particle and repeat the random walk.
6. After a perimeter site is contacted m times, the site is filled and new perimeter sites are identified. The scores (number of contacts) associated with these sites



Fig. 2. Representative cluster of 21888 particles with $\alpha = 0.2$ $m = 1$. It shows a fractal pattern.

are set to zero. This is the so-called noise reduction technique, it decreases the noisiness of the cluster for large value of m . In the limit of infinite m , the simulation would correspond to a solution of Laplace equation (1) to (3), without any fluctuations in micro-scale.

Owing to the screen effect of the growing part, the aggregate grows into a tree-like pattern for small value of m . Figure 2 shows a cluster consisting of 21888 particles with $m = 1$ and $\alpha = 0.2$. Figure 3 shows a cluster with the same alpha as before but with $m = 50$, the noise is now much repressed and lattice anisotropy shows up. One can compare the experimental Picture 6 with the pattern in Figure 2.

Next the value of alpha is changed to a larger value of 0.4. This would correspond to a smaller surface tension effect. Figure 4 shows the time evolution of every other 2000 particles, that is, the dark and white stripes all contain 2000 particles. First, we notice that the structure becomes more dendrite-like compared to Figure 3. The initial first 2000 clusters is very much space-filling but as the cluster becomes much larger the cluster attains its asymptotic dendrite structure¹⁹⁻²⁰. Figure 4 can be compared with the structure observed in Picture 1 nicely.

Finally, when the value of alpha is increased to 0.6 with $m = 50$, one can see in Figure 5 that the dendrite becomes more needle-like, the side chain becomes much repressed. We find again that an decreased surface tension results in



Fig. 3. Same as Figure 2 but with $m = 50$. The structure becomes much less noisy, and the side branches are much repressed.

cluster with thinner fingers and with a smaller compact center¹⁹⁻²⁰. The large value of noise reduction parameter m here serves to encourage the anisotropic growth along lattice direction. This is often observed in the case of vapor condensation of water with large supercooling although our sample of Camphene apparently does not show this pattern.

Due to the fact that real crystal shows anisotropic surface tension, real molecules are not spherical and molecular diffuses on solid surface. The present simulation is probably not very realistic. However, it is our purpose is

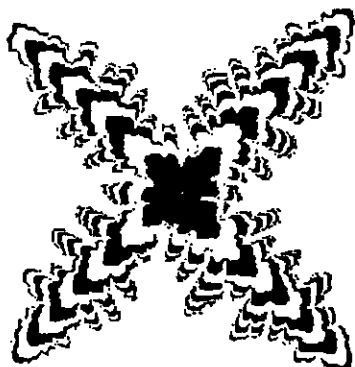


Fig. 4. Cluster of 20908 particles with $\alpha = 0.4$ and $m = 50$, the dark and white stripes all contain 2000 particles. The initial first 2000 cluster is very much space-filling but as the cluster becomes much larger the cluster attains its asymptotic dendrite structure.

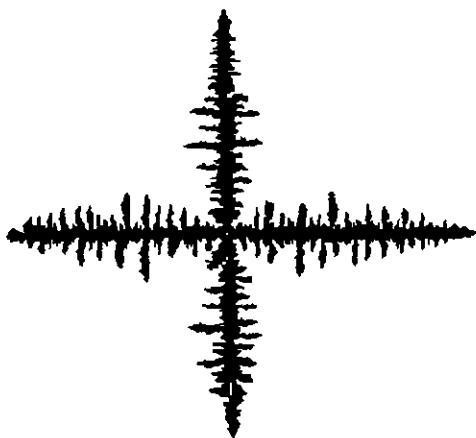


Fig. 5. Cluster of 7870 particles with $\alpha = 0.6$ and $m = 50$, the structure becomes more needle-like.

to show that one can indeed understand the global patterns in phase transformation. At present, it is still not clear that one can understand the mesoscale patterns by using the basic idea in DLA model. One has to study more closely the matter by both experimental and computational approaches. The present work serves to demonstrate that the combination of computer-enhanced Video-microscopic and simulation is a powerful tool in the study of non-equilibrium structures.

ACKNOWLEDGMENT

This research was supported by a grant from National Science Council. (Grant no. NSC-77-0208-M002-17)

Received November 1, 1989.

Key Word Index-

Nonequilibrium pattern; Diffusion Limited Aggregates; Crystal Growth; Video-microscopy.

REFERENCES

1. Spencer, M., "Fundamentals of light microscopy" 1982, Cambridge U.Press.
2. Walter, R.J. and Berns, M.W. *Proc. Nat. Acad. Sci.* 1981, 78, 6927.
3. Allen, R.D. (a) *Scientific American*. 1987, February. (b) *Ce Motil.* 1981, 1, 275.
4. Tanaka, H.; Hayashi, T. and Nishi, T., (a) *J. Appl. Phys.* 1986, 59, 653. (b) *ibid.* 1986, 59, 3627. (c) *Phys. Rev. Lett.* 1987, 59, 692.
5. (a) Kachar, B.; Evans D.F. and Evans, B.W., *J. Colloid interface Sci.* 1984, 100, 287. (b) Benton, W.J.; Raney, K.H. and Miller, C.A. *J. Colloid interface Sci.* 1986, 110, 363.
6. Mueller, S.C.; Plesser, T. and Hess, B. *Naturwissenschaften*

- ten 1986 73, 165.
7. Mueller, S.C.; Plesser, T. and Hess, B. *Physica* 1987, 4D, 71.
 8. Hiraoka, Y.; Sedat, J.W. and Agard, D.A. *Science* 1987, 238, 36.
 9. Langer, J.S. "Lecture in Theory of Pattern Formation" in "Chance and Matter" ed. by J. Souletie et al. 1987 Elsevier, Amsterdam.
 10. Kessler, D.A.; Koplik, J. and Levine, H. *Adv. Phys.* 1988, 37, 255.
 11. Huang, S-C; and Glicksman, M.E. *Acta Metallurgica* 1981, 29, 701.
 12. Mullins, W.W.; and Sekerka, R.F. *J. Appl. Phys.* 1963, 34, 323.
 13. Inoue, S. "Video Microscopy" 1986, Plenum.
 14. Gonzalez, S.C. and Wintz, "Digital Imaging Processing" 1987, 2nd. Ed. Addison-Wesley.
 15. Nittmann, J. and Stanley, H.E. *Nature* 1986, 321, 663.
 16. Witten, T.A. and Sander, L.M. *Phys. Rev. Lett.* 1981, 47, 1400.
 17. Vicsek, T. "Fractal Growth Phenomena", 1989, World Scientific, Singapore.
 18. Witten, T.A. and Sander, L.M. *Phys. Rev.* 1983, B27, 5686.
 19. Tao, R.; Vovotny, M.A. and Kaski, K. *Phys. Rev.* 1988, A38, 1019.
 20. Aukrust, T.; Novotny, M.A.; Browne, D.A. and Kaski, K. *Phys. Rev.*, 1989, A39, 2587.

